Available online at www.sciencedirect.com

SciVerse ScienceDirect

Procedia Computer Science 18 (2013) 1969 – 1978

Procedia Computer Science

International Conference on Computational Science, ICCS 2013

Issues Related to Parameter Estimation in Model Accuracy Assessment

Thomas C. Henderson*, Narong Boonsirisumpun

University of Utah, Salt Lake City, Utah, USA

Abstract

Model Accuracy Assessment (MAA) is an important part of the modern verification and validation process. This involves not only evaluation of a validation metric comparing experimental versus simulation system response quantities, but also the determination of the adequacy of the model for its intended use (see [1] for a detailed description). We describe here some issues related to the use of parameter estimation on MAA in the study of heat flow in a 2D metal plate. We consider seven parameter estimation techniques, and show that various factors such as length of sampling time, parameter estimation method, etc. impact the MAA. The ultimate goal is to improve MAA techniques in aircraft structural health care monitoring using Bayesian Computational Sensor Networks.

Selection and peer review under responsibility of the organizers of the 2013 International Conference on Computational Science

Keywords: Model Accuracy Assessment, Validation, Parameter Estimation, Prediction

1. Introduction

The major specific objectives of our work are to:

1. Develop Bayesian Computational Sensor Networks (BCSN) which detect and identify structural damage. We aim to quantify physical phenomena and sensor models; e.g., develop piezoelectric and other computational models to reconstruct physical phenomena and characterize uncertainties due to environmental factors.
2. Develop an active feedback methodology using model-based sampling regimes (rates, locations and types of data) realized with embedded sensors and active sensor placement. This will allow on-line sensor model validation, and the use of on-demand complimentary sensors.
3. Develop a rigorous model-based systematic treatment of the following uncertainty models: (1) stochastic uncertainties of system states, (2) unknown model parameters, (3) dynamic parameters of sensor nodes, and (4) material damage assessments (viewed as source input parameters).

*T.C. Henderson. Tel.: +1-801-581-3601 ; fax: +1-801-581-5843 .
E-mail address: narong.boonsirisumpun@utah.edu (N. Boonsirisumpun), tch@utah.cs.edu (T.C. Henderson).

1877-0509 © 2013 The Authors. Published by Elsevier B.V.
Selection and peer review under responsibility of the organizers of the 2013 International Conference on Computational Science
doi:10.1016/j.procs.2013.05.366

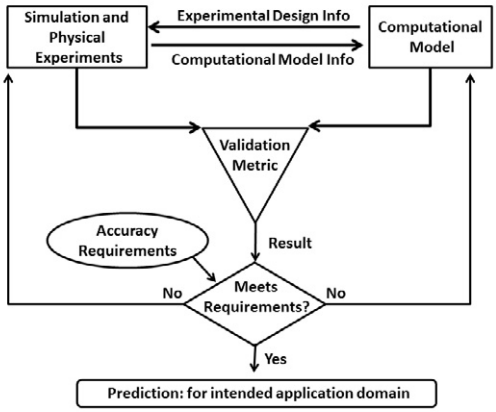

Fig. 1. Model Accuracy Assessment (based on Fig. 12.4 from [1]).

This work addresses 3 of the 4 DDDAS (Dynamic Data-Driven Analysis Systems) interdisciplinary research components: applications modeling, advances in mathematics and statistical algorithms, and application measurement systems and methods, and more specifically addresses several questions raised in the DDDAS-InfoSymbiotics 2010 Report [2] by Working Group 3 (WG3) Large and Heterogeneous Data from Distributed Measurement & Control Systems (Alok Chaturvedi, Adrian Sandhu): "DDDAS inherently involves large amounts of data that can result from heterogeneous and distributed sources which require analysis before automatically integrating them to the executing applications that need to use the data."

The incorporation of efficient and scalable probabilistic methods into model-based simultaneous state estimation and parameter identification may have a large impact on the exploitation of spatially distributed sensing and computation systems throughout a wide range of scientific domains. Spatially distributed physical phenomena such as temperature, wave propagation, etc., require observation with dynamically located sensors in order to achieve better tuned computational models and simulations. Methods developed here allow for online validation of models through direct sensor observation. Significant problems which must be overcome include the interpolation between measurement data, as well as the estimation of quantities which cannot be directly measured (e.g., thermal diffusivity coefficients). The demonstration of how stochastic partial differential equations can be used to this end should have strong impact on practice in many applications, including the aircraft Structural Health Monitoring (SHM) problem. Our major goal is to provide rigorous Bayesian Computational Sensor Networks to quantify uncertainty in (1) model-based state estimates incorporating sensor data, (2) model parameters (e.g., diffusivity coefficients), (3) sensor node model parameter values (e.g., location, bias), and input source properties (e.g., locations and extent of cracks). This is achieved in terms of extensions to our recently developed techniques (see [3, 4, 5]). We call this approach *Bayesian Computational Sensor Networks* (BCSN). These decentralized methods have low computational complexity and perform Bayesian estimation in general distributed measurement systems (i.e., sensor networks). A model of the dynamic behavior and distribution of the underlying physical phenomenon is used to obtain a continuous form from the discrete time and space samples provided by a sensor network. Others have recently begun to explore the Bayesian approach for computational simulation [6, 7, 8]. For example, Tinsley [9, 10] proposes "the systematic treatment of model and data uncertainties and their propagation through a computational model to produce predictions of quantities of interest with quantified uncertainty." The approach is applied to tumor modeling and analysis. Another related work is that of Furukawa [11] who takes location uncertainty into account when localizing defects and "formulates the uncertainties of sensor states stemming from both motion and measurement and allows stochastic identification of defects using recursive Bayesian estimation."

The first step in our project is to extend to 2D the existing 1D *Bayesian Computational Sensor Networks* approach to heat flow and establish the adequacy of the approach on a simpler problem than ultrasound. Here we

describe the impact of parameter estimation on MAA in this context. Figure 1 shows the validation, calibration and prediction process as described by Oberkampf [1]. Experiments are used to establish parameters in the computational model, and these in turn affect the result of the validation metric. Both simulation experiments and physical experiments are used to help with experiment design as well as to inform the computational modeling process. When studying parameter estimation methods in simulation experiments, implicit methods are used to represent the phenomenon, whereas an explicit method is used in the method (e.g., EKF update formulas are based on the explicit time step function at each location). These simulation experiments provide information as to the feasibility and truncation error affects of the explicit method based computational model. Here we perform a comparison of seven parameter estimation approaches (Inverse method, LLS, MLE, EKF, Particle Filter, Levenberg-Marquardt, Minimum RMS error) to estimate the value of thermal diffusivity (k) in heat flow in a 2D plate. The comparison is made in terms of the adequacy requirements. The major question raised is whether the statistics produced by the parameter estimation techniques can be used to characterize the adequacy of the model. Secondary questions include: (1) Which method gives the best k estimate? (2) Which is least sensitive to noise? and (3) Which method has lowest time complexity?

2. Method

The 2D heat conduction equation is given as:

$$\frac{\delta T}{\delta t} = k(\frac{\delta^2 T}{\delta x^2} + \frac{\delta^2 T}{\delta y^2}) \tag{1}$$

where T is temperature, t is time, δx, δy are space in x,y respectively and k is thermal diffusivity. We use the explicit method that has a forward finite difference to approximate the time derivative

$$\frac{\delta T}{\delta t} = \frac{T^{t+1}_{x,y} - T^t_{x,y}}{\Delta t} \tag{2}$$

The second derivative in space is represented by the 2D Laplacian:

$$\frac{\delta^2 T}{\delta x^2} + \frac{\delta^2 T}{\delta y^2} = \frac{T^t_{x-1,y} - 2T^t_{x,y} + T^t_{x+1,y}}{\Delta x^2} + \frac{T^t_{x,y-1} - 2T^t_{x,y} + T^t_{x,y+1}}{\Delta y^2} \tag{3}$$

Substituting equations (2) and (3) into (1), we have,

$$\frac{T^{t+1}_{x,y} - T^t_{x,y}}{\Delta t} = k(\frac{T^t_{x-1,y} - 2T^t_{x,y} + T^t_{x+1,y}}{\Delta x^2} + \frac{T^t_{x,y-1} - 2T^t_{x,y} + T^t_{x,y+1}}{\Delta y^2}) \tag{4}$$

The truncation error for this is [1]:

$$TE_h(T) = [\frac{1}{2}\frac{\partial^2 T}{\partial t^2}]\Delta t + [\frac{-k}{12}\frac{\partial^4 T}{\partial x^4}](\Delta x)^2 + O(\Delta t^2, \Delta x^4)$$

or $TE = O(\Delta t, \Delta x^2)$ where h characterizes convergence (i.e., $h = \frac{\Delta x}{\Delta x_{ref}} = \frac{\Delta t}{\Delta t_{ref}}$ so that when $h \to 0$, then $\Delta x, \Delta t \to 0$ at the same rate). From Equation (4) the value of k at each location (x, y) is

$$k = \frac{T^{t+1}_{x,y} - T^t_{x,y}}{\Delta t(\frac{T^t_{x-1,y} - 2T^t_{x,y} + T^t_{x+1,y}}{\Delta x^2} + \frac{T^t_{x,y-1} - 2T^t_{x,y} + T^t_{x,y+1}}{\Delta y^2})} \tag{5}$$

When $\Delta x^2 = \Delta y^2$, this is rewritten as:

$$k = \frac{\Delta x^2 (T^{t+1}_{x,y} - T^t_{x,y})}{\Delta t(T^t_{x-1,y} + T^t_{x+1,y} + T^t_{x,y-1} + T^t_{x,y+1} - 4T^t_{x,y})} \tag{6}$$

From Equation (6), we can calculate the value of k at every spatial location (x, y) and every time step (t) but it gives a wide range of k values with high variance. Thus, we use the average value of k over the entire set of inverse calculations. We also compare the accuracy, noise sensitivity and time efficiency of the methods.

2.1. Inverse method

The first estimation method we study is what we call the Inverse method which solves for the value of k at each (x, y) from (6) and then finds the average of all k values. This method estimates a global k value as the mean of the local k values.

$$k_{est} = \frac{\sum k_{x,y,t}}{N}$$

where x, y is the location, t is time step (t = 2...max_t) and N is number of k values.

2.2. LLS (Linear Least Squares)

The second estimation method we used is LLS (linear least squares). This approach finds the line that best fits the data (with minimum sum of the squares of the residual). We can rewrite Equation (4) as:

$$C \cdot k = d$$

where C is the Laplacian term and d is the time derivative term, and the LLS method gives the estimate of k as:

$$k_{est} = \min_k \|C \cdot k - d\|^2$$

2.3. MLE (Maximum Likelihood Estimation)

The third method is MLE (maximum likelihood estimation). By taking the derivative of the log likelihood function of T, the MLE will give the estimate of k as (again assuming $\Delta x^2 = \Delta y^2$):

$$k_{est} = \frac{\Delta x^2 \sum((T^{t+1}_{x,y} - T^t_{x,y})(T^t_{x-1,y} + T^t_{x+1,y} + T^t_{x,y-1} + T^t_{x,y+1} - 4T^t_{x,y}))}{\Delta t \sum(T^t_{x-1,y} + T^t_{x+1,y} + T^t_{x,y-1} + T^t_{x,y+1} - 4T^t_{x,y})^2}$$

2.4. EKF (Extended Kalman Filter)

The fourth method is to add the k parameter to the state estimate of an EKF (for more on the Kalman filter, see Thrun et al. [12]). Given the equation for heat flow above, we have the equation for the temperature state evolution as:

$$\dot{x}_i(t) = k\frac{\delta^2 T}{\delta x^2}$$

where i = 1...n; then add the equation for the thermal diffusivity parameter:

$$\dot{x}_{last} = 0$$

which arises from the next state equation:

$$k_{t+1} = k_t + \epsilon$$

where ϵ is sampled from a normal distribution with variance σ^2_p. Finally, reformulating for one position between the 4-neighbors, we have:

$$x_t = g(x_{t-1}) + \epsilon_t$$

$$z_t = h(x_t) + \delta_t$$

where

$$g_i : x_{i,t} = x_{i,t-1} + \frac{\delta t(x(i_1, t-1) + x(i_2, t-1) + x(i_3, t-1) + x(i_4, t-1) - 4x_{i,t-1})}{\delta x^2} x_{last,t-1} + \epsilon_{i,t}$$

$$g_{last} : x_{last,t} = x_{last,t-1} + \epsilon_{last,t}$$

2.5. Particle Filter (Sequential Monte Carlo)

The fifth method is the Particle Filter. By sampling the p particles set from the range of the probability distribution, a weight function is used to recalculate the probability of each particle, and then re-sampling occurs to obtain a set of particles from the new probability distribution. This is repeated until the change in the range of the particle value is small enough.

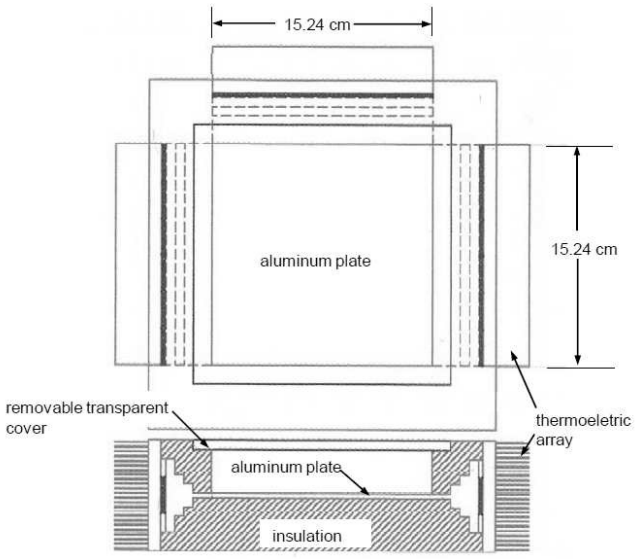

Fig. 2. Experimental Apparatus Layout.

2.6. Levenberg-Marquardt

The sixth method is Levenberg-Marquardt (see Ozisik [13]). The Levenberg-Marquardt allows estimation of the thermal diffusivity at each location by using the iterative estimation method of the Jacobian:

$$J = \frac{\delta T}{\delta \hat{k}} = \begin{pmatrix} \frac{\delta \hat{T}_1}{\delta \hat{k}_1} & \frac{\delta \hat{T}_1}{\delta \hat{k}_2} & \cdots & \frac{\delta \hat{T}_1}{\delta \hat{k}_n} \\ \frac{\delta \hat{T}_2}{\delta \hat{k}_1} & \frac{\delta \hat{T}_2}{\delta \hat{k}_2} & \cdots & \frac{\delta \hat{T}_2}{\delta \hat{k}_n} \\ \vdots & \vdots & \ddots & \vdots \\ \frac{\delta \hat{T}_m}{\delta \hat{k}_1} & \frac{\delta \hat{T}_m}{\delta \hat{k}_2} & \cdots & \frac{\delta \hat{T}_m}{\delta \hat{k}_n} \end{pmatrix}$$

where $\hat{k}$ is set of unknown thermal diffusivity values in each location $[k_1, k_2, ...k_n]$; the Levenberg-Marquardt solves for $\hat{k}$ as:

$$\hat{k}^{i+1} = \hat{k}^i + (J^T J + \mu_i I)^{-1} J^T (Y - T)$$

where μ_i is the positive damping parameter and $i = 1, 2, 3, ...$ Levenberg-Marquardt converges when $|\hat{k}^{i+1} - \hat{k}^i| < \epsilon$.

2.7. Minimum RMS Error

Another way to estimate the thermal diffusivity is to use the RMS error by simply searching the value of k that gives the minimum RMS error (over some range of possible k values).

$$k_{est} = \min_k \|RMS_{error}\|$$

This method should guarantee that we find the k value that has the minimum RMS error.

2.8. Comparison of Methods

In order to compare the methods, we use both simulated and experimental heat flow data through a 2D plate. The layout of the experimental apparatus is shown in Figure 2. A FLIR T420 high performance IR camera takes a 320x240 pixel array, of which a 170x170 subset samples the aluminum plate. Figure 3 shows an example image with heat sources on the left and upper parts of the plate. In order to get smoother results in the parameter estimation methods, the image is averaged down to a 17x17 grid. Δt is set to $30sec$ with $max\_t = 59x30 = 1770$,

Fig. 3. Example IR Image of the Aluminum Plate.

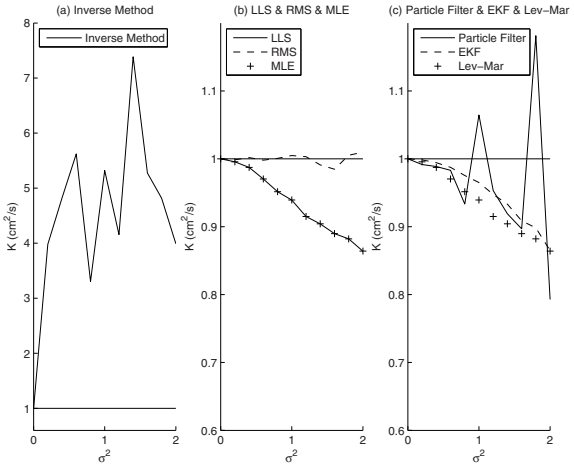

Fig. 4. k Estimate Results with Noise in the Data.

and $\Delta x = \Delta y = 15.24/17$ cm (in simulation experiments, k is set to 0.85. The sample set is then Tn with time step $t = 1, 2, 3, ...58$:

$$Tn = T(x, y, 1 : t + 1)$$

In simulation experiments, we use the testing data Tn to run experiments for the seven estimation methods to get the value of k over 30 trials for each method. The error of the k estimation is compared between the 7 methods according to the equation:

$$k_{error} = \frac{||k - k_{est}||}{k}$$

Note that this corresponds to finding the computational model parameter. We then use the k estimate to run a new temperature simulation $S(x, y, t)$ with the simulated temperature at location (x, y) and time t, and compute the RMS (Root Mean Square) error:

$$RMS_{error} = \sqrt{\frac{\sum(T_{x,y,t} - S_{x,y,t})^2}{N}}$$

where N is the number of locations time the numbers of time step - 1. This is how adequacy of the model is determined.

3. Verification

Chapra [14] gives an example of heat flow simulation, and our 2D implicit forward simulation gives a solution which matches that given in the book. To verify the parameter estimation methods, heat flow is simulated under these conditions (with no added noise), and all methods produce the value of k used in the simulation. The affect of noise on the parameter estimation methods was also investigated, and the results are shown in Figure 4.

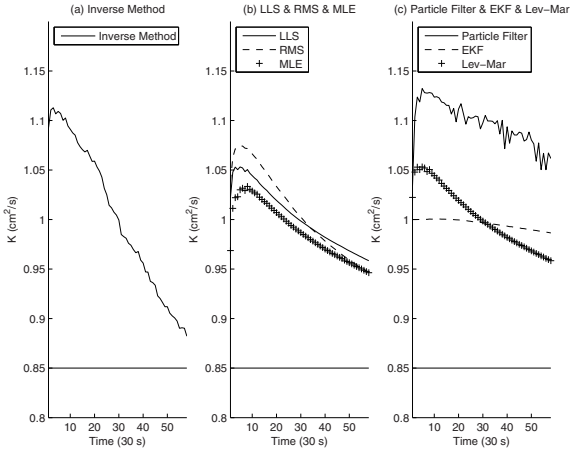

Fig. 5. k Estimate Results.

4. Data

Figure 5 shows the results of the physical experiments for thermal diffusivity estimation using the seven methods. The x-axis corresponds to the time step, and the k estimate at each time step is that found with all the data up to that time. The error in the k estimates of the seven methods is shown in Figure 6.

Using the means and variances found for each of the seven methods, their Gaussian distributions are shown in Figure 7. Figure 8 shows the RMS error for the temperature sequences produced with the respective k values of the seven methods. The time cost for the seven methods is shown in Figure 9.

Finally, Figure 10 shows the temperature predictions for the various parameter estimation methods. It is clear that estimates all result a sequence which diverges from the actual data.

5. Analysis

The error of k estimation across the seven methods can be seen in Figures 5 and 6. Here we have assumed that the actual value of k is 0.85. All of these methods produce a mean and a variance for the k estimate, and this allows some amount of confidence in each result (note, however, that an estimation technique that returns a constant would have zero variance!). We also see that it may be better to combine the estimates in order to better estimate the computational parameter (in this case thermal diffusivity). The methods produce similar results, but the spread in k estimate is about 0.2. The plots in Figure 7 for the k a posteriori distributions give a qualitative view of the results.

Assume that the accuracy requirements are imposed as a specified level of RMS error between the model prediction and experimental data. Then an interesting aspect of the RMS error shown in Figure 8 is that meeting the accuracy requirements depends on the length of the time sequence used (shorter ones will succeed but longer will fail). Note that the RMS error does not settle down to a fixed level; this may occur due to the overall misfit of the model (the physical world is more complicated than the model), or may happen as the temperature converges to a steady state (in which case the time derivative is zero). All these surrounding conditions play a role in the exploitation of this model and need to be considered in any application as well.

Figure 9 shows the time cost of the methods. The results show that on this dataset PF is the most costly, followed by EKF, LLS, Levenberg-Marquardt, the Minimum RMS, Inverse method and MLE is the least costly method.

6. Conclusions and Future Work

The results here show that a variety of factors impact the use of experimental data in determining computational model parameters as far as assessing model adequacy. Thus, a broader set of considerations must be addressed

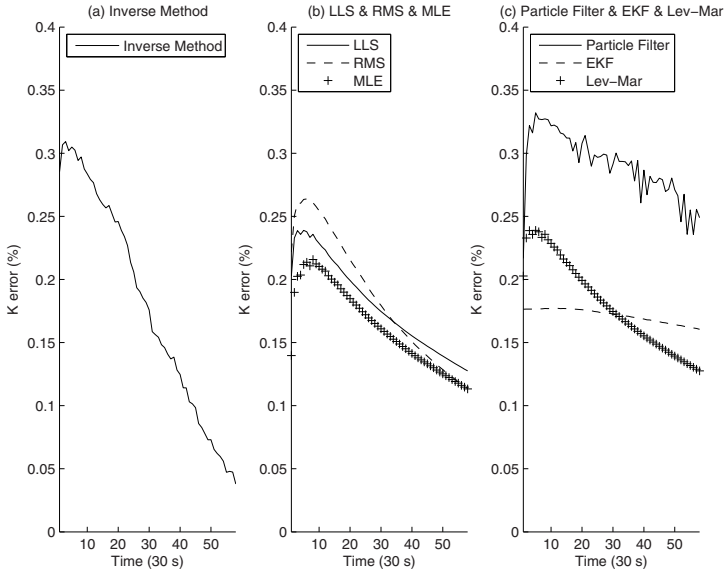

Fig. 6. *k* Estimate Error.

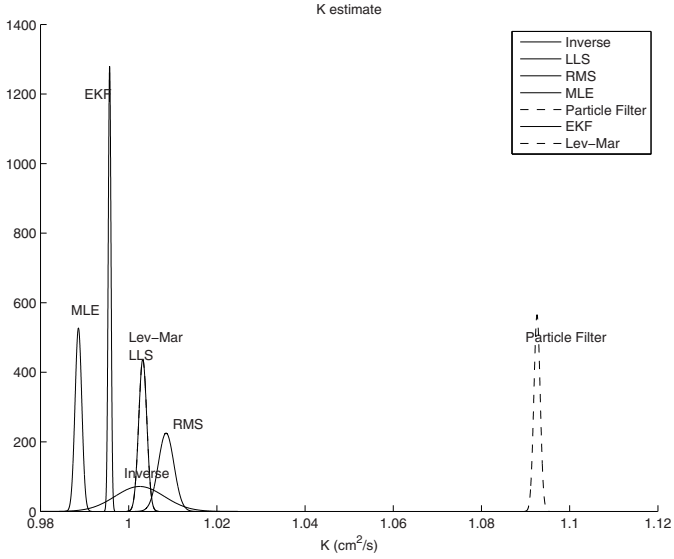

Fig. 7. The Gaussian Distributions for the *k* Estimates.

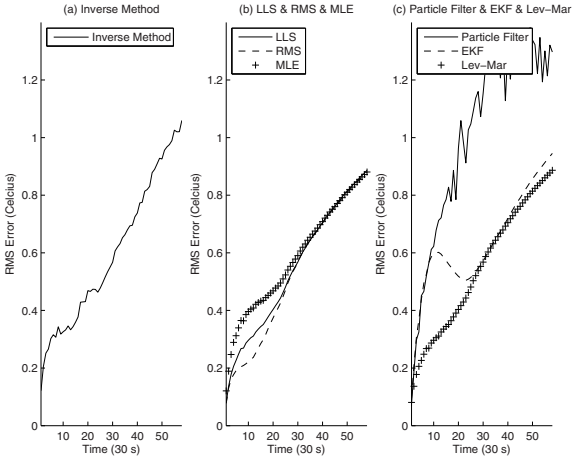

Fig. 8. RMS Error of Temperature Sequences for the Parameter Estimation Methods.

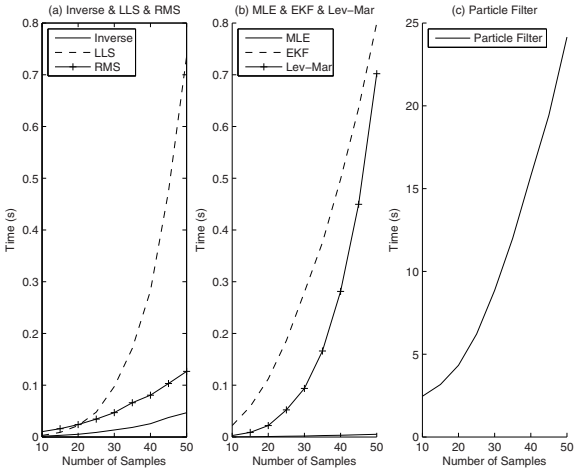

Fig. 9. Time Cost of Methods.

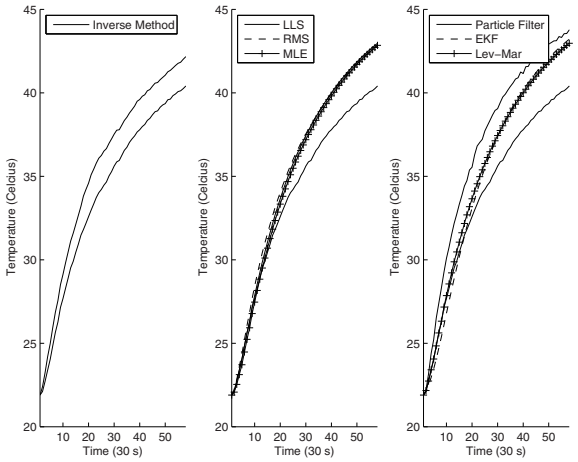

Fig. 10. Temperature Predictions vs. Experimental Data.

for every specific application. For temporal data, this includes the number of time steps considered as well as the parameters of the simulation. For example, even though the experimental data is sampled at time steps of 30 seconds, the simulation must be run with a much smaller time step (say $\Delta t = 0.1$ second). These results will be used to establish the appropriate framework for model validation in the structural health problem; that is, how to structure built-in model validation methods for use in a dynamical data-driven analysis system.

We have also compared seven thermal diffusivity estimation methods: Inverse Method, LLS, MLE, Minimum RMS, EKF, PF, and Levenberg-Marquardt. The results show that the methods produce fairly consistent results, and in fact, a combination may provide a better estimate.

We are currently working on a more comprehensive set of experiments, and will be able to comment on the predictive aspect of the computational model in future work. In addition, the uncertainty in other input parameters to the computational model need to be studied, including Δx (the locations of the pixels on the actual metal plate are uncertain), Δt (the sample times also have some amount of uncertainty), boundary conditions, etc.

Of course, this work constitutes the first-round study to establish a framework for an in-depth analysis of the use *Bayesian Computational Sensor Networks* for aircraft structural health determination using ultrasound. We are currently developing computational models for this, as well as setting up an experimental framework. We look forward to reporting on these in future meetings.

Acknowledgments This work was supported by AFOSR-FA9550-12-1-0291.

We like to acknowledge Jeff Kessler's help in gathering experimental data, and other project members (John Mathews, Dan Adams, Eddie Grant, and Sabita Nahata) for their input on this and related material.

References

[1] W. Oberkampf, C. Roy, Verification and Validation in Scientific Computing, Cambridge University Press, Cambridge, UK, 2010.
[2] C. Douglas, A. Patra, AFOSR/NSF Workshop on Dynamic Data Driven Application systems, unpublished report (October 2011).
[3] T. Henderson, Computational Sensor Networks, Springer-Verlag, Berlin, Germany, 2009.
[4] F. Sawo, T. Henderson, C. Sikorski, U. Hanebeck, Sensor Node Localization Methods based on Local Observations of Distributed Natural Phenomena, in: Proceedings of the 2008 IEEE International Conference on Multisensor Fusion and Integration for Intelligent Systems (MFI 2008), Seoul, Republic of Korea, 2008.
[5] F. Sawo, Nonlinear State and Parameter Estimation of Spatially Distributed Systems, Ph.D. thesis, University of Karlsruhe (January 2009).
[6] H. Massard, O. Fudym, H. Orlande, J. Batsale, Nodal Predictive Error Model and Bayesian Approach for Thermal Diffusivity and Heat Source Mapping, C.R. Mecanique 338 (2010) 434–449.
[7] J. Wang, N. Zabaras, Using Bayesian Statistics in the Estimation of Heat Source in Radiation, Intl. Jnl of Heat and Mass Transfer 48 (2005) 15–29.
[8] J. Wang, Bayesian Computational Techniques for Inverse Problems in Transport Processes, Ph.D. thesis, Cornell University, Cornell, NY (January 2006).
[9] A. Hawkins-Daarud, S. Prudhomme, K. van der Zee, T. Oden, Bayesian Calibration, Validation, and Uncertainty Quantification of Diffuse Interface Models of Tumor Growth, Tech. Rep. ICES Report 10-44, University of Texas (November 2010).
[10] T. Oden, R. Mosner, O. Ghattas, Computer Predictions with Quantified Uncertainty, Tech. Rep. ICES Report 10-39, University of Texas (October 2010).
[11] T. Furukawa, J. Cheng, S. Lim, F. Xu, R. Shioya, Defect Identification by Sensor Network Under Uncertainties, in: Proceedings of the 2010 International Conference on Broadband, Wireless Computing, Communication and Applications, BWCCA '10, IEEE Computer Society, Washington, DC, USA, 2010, pp. 155–158.
[12] S. Thrun, W. Burgard, D. Fox, Probabilistic Robotics, MIT Press, Cambridge, MA, 2005.
[13] M. Ozisik, Heat Conduction, 2nd ed., John Wiley, New York, 1993.
[14] S. Chapra, R. Canale, Numerical Methods for Engineers, McGraw-Hill, Boston, MA, 2010.